# An accurate method for measuring the dielectric constant of printed wiring board materials

**N.G. Paulter**
Electricity Division, National Institute of Standards and Technology, Gaithersburg, Maryland, USA

**Keywords**
Printed circuit boards, Dielectric constants

**Abstract**
A new time-domain reflectometry measurement method is described that provides accurate measurements of the average high-frequency (0.1GHz - 10GHz) dielectric constant of printed wiring board materials and is suitable for "factory floor" use. A parallel-plate transmission line is used for the sample geometry. Only simple numerical processes are required to extract the characteristic impedance and dielectric constant of the sample from the acquired data. The long-term measurement reproducibility and short-term measurement repeatability of the method are described.



**The author would like to thank G.W. Smedley III of Texas Instruments, Austin, TX; R.M. Japp of IBM Microelectronics, Endicott, NY; B. Holmes of Lucent Technologies, Richmond, VA; and T.A. Zawislak of Arlon, Dear, DE for providing PWB samples. The author is also grateful to R.H. Palm of NIST, Gaithersburg, MD for preparing the samples; D.R. Larson and D.W. Berning of NIST Gaithersburg, MD for technical comments and discussions; B.A. Bell of NIST, Gaithersburg, MD for administrative and editorial support; and the Advanced Technology Program of NIST for supporting this work. This paper has been printed from the *Proceedings of the Technical Conference, IPC Printed Circuits Expo '99*, Long Beach, CA, USA.**

Circuit World
26/1 [1999] 27–32
MCB University Press
[ISSN 0305-6120]

## 1. Introduction

A time-domain reflectometry (TDR) measurement method has been recently reported for measuring the average high-frequency (0.1GHz - 10GHz) relative dielectric constant (real part of the relative complex permittivity), $\epsilon'_r$, of printed wiring board (PWB) materials (Paulter, 1996; 1998). PWBs are used as substrates on which integrated circuits and discrete electronic devices are mounted and electrically connected. These electrical connections, or interconnects, may behave as transmission lines (TLs) in high-speed/high-frequency applications thus making the electromagnetic wave propagation properties of the interconnect important. The electrical properties of the PWB TLs are dependent on a variety of variables that include dielectric and conductor properties and the physical dimensions of the TLs. This work focuses on a measurement method for determining $\epsilon'_r$ and, in particular, on a method for obtaining the average high-frequency (0.1GHz - 10GHz) value of $\epsilon'_r$. An average value is sought because a scalar is typically all that is used for PWB circuit design and $\epsilon'_r$ is fairly constant for most PWB dielectrics over this frequency range.

Although a variety of frequency-domain (for example, Lightart, 1983; Kent, 1991; Stuchly *et al.*, 1994; Baker-Jarvis *et al.*, 1993) and time-domain (for example, Fellner-Feldegg, 1969; Nicolson and Ross, 1970; Cole, 1975; Boned and Peyrelasse, 1982) methods have been developed for determining $\epsilon'_r$, this method addresses measurement requirements unique to the PWB industry, namely: that the measurement system be an inexpensive, easy to use, robust "factory floor" system, and allow for quick and easy sample preparation. The measurement method described here addresses the unique PWB requirements by affording simple sample fabrication (no chemical or photolithographic process) and fast data acquisition and parameter extraction (under three minutes to acquire the sample and reference data), and because it is inexpensive and easy to use (TDR-capable oscilloscope), accurate (agreement with frequency-domain methods is better than 1 per cent), and robust (insensitive to position of sample in sample holder). These attributes make the method suitable for both the laboratory and factory floor environments. This work also addresses anecdotal claims of an apparent discrepancy between the results obtained using time-domain and frequency-domain methods. For materials that are dielectrically anisotropic, such as most PWB materials, the dielectric sample must be aligned properly with respect to the applied electric field to measure the $\epsilon'_r$ that is experienced by a wave propagating along a PWB TL. The sample geometries used here ensure the proper orientation.

## 2. Experimental

### 2.a. Measurement system

The measurement system uses an equivalent-time, nominally 50Ω input impedance, TDR-capable, sampling oscilloscope and a computer controller to obtain the reflection coefficient data from which $\epsilon_r$ is extracted (to be discussed later). In the TDR mode, the oscilloscope delivers a rectangular voltage pulse to the sample and then records the pulse that is reflected from the sample. The reflected pulse is a consequence of the impedance discontinuity between the oscilloscope and the sample and, therefore, provides a measurement of the sample's impedance from which $\epsilon_r$ is extracted. The TDR signal that is observed is represented by the trace shown in Figure 1. The duration of the steps in Figure 1 corresponds to the round-trip propagation time of the TL. The amplitude of the steps reflects the impedance discontinuities between the TL and the oscilloscope and between the TL and its termination. For this work, the termination is an open circuit and only the first reflected step is used.

### 2.b. Sample

The sample is a parallel-plate transmission line (PPTL) structure (see Figure 2). Sample preparation for the PPTL is extremely simple. A TL of length, L, having a uniform width, W, is removed (by a shear or router) from a sheet of

Figure 1
Idealized TDR signal

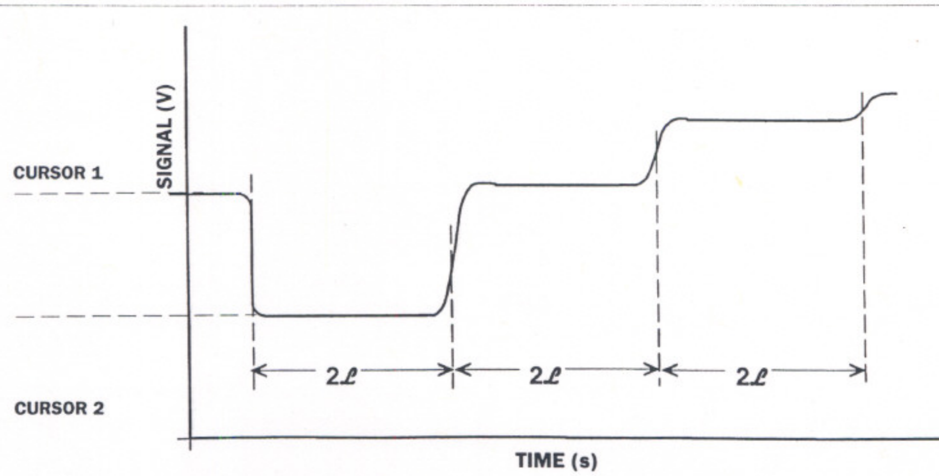

**Figure 2**
Schematic of PWB sample. The width of the sample is given by W, the length by L, the total thickness by $t_T$, the dielectric thickness by $t_d$, and the conductor thickness by $t_m$

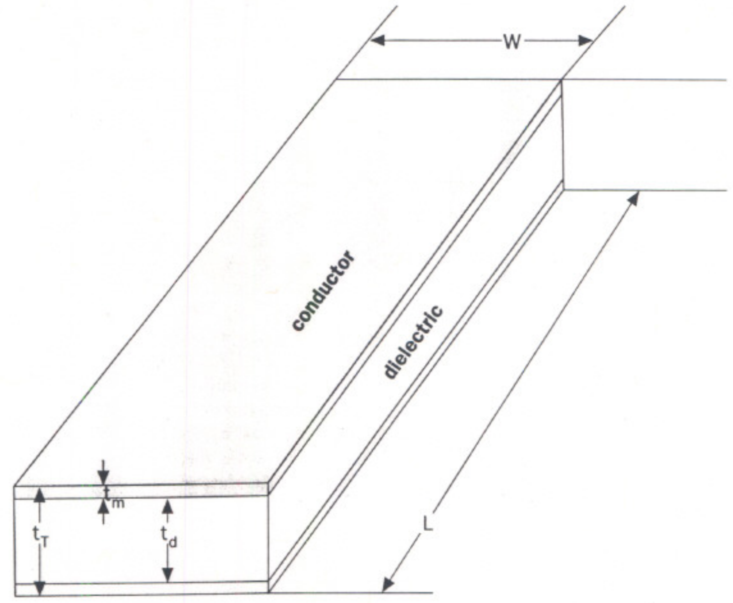


**Figure 3**
Schematic of PWB sample holder with sample in place. The sample is tilted 2° from the perpendicular to exaggerate the effect of tilt on sample electrical contact

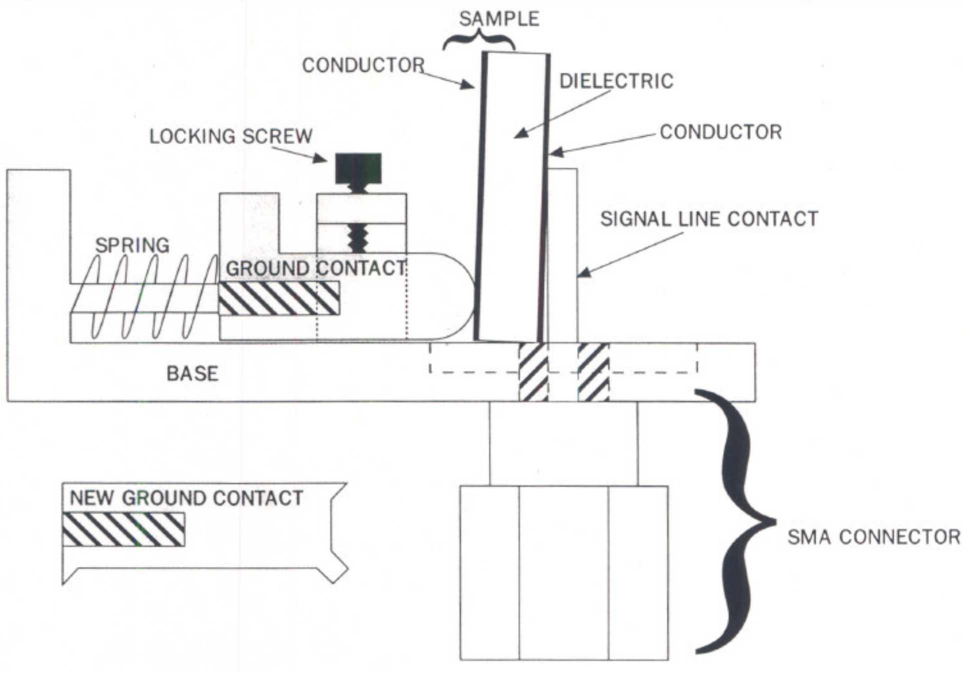


laminate. Both sides of the laminate must be metal clad. The sample is prepared so that the long edges of the PPTL are as parallel as possible. Deviations from being parallel increase the measurement uncertainty. The edges are deburred to ensure that the electric field is uniform along the length of the samples. To facilitate handling, sample widths of approximately 1.25cm were used. The lengths of the samples were long enough so that line lengths did not affect the measured signal (Paulter, 1996).

### 2.c. Sample holder

The measurement results presented here were taken using three different sample holder designs, SH1, SH2, and SH3. SH2 and SH3 are shown in Figure 3; SH3 incorporates a ground contact with knife edges. SH1 is described in Paulter (1996) and is a SMA-connectorized PWB receptacle with four solder tabs, one on each corner. Design improvements resulted in improved measurement reproducibility and repeatability.

### 2.d. Extraction of $\epsilon'_r$

The $\epsilon'_r$ of the sample is extracted from the PPTL impedance, $Z_T$. The $Z_T$ is obtained from the TL reflection coefficient, ρ,

$$\rho = \frac{Z_T - Z_0}{Z_T + Z_0}, \quad (1)$$

where $Z_0$ is the input impedance of the oscilloscope. Solving for $Z_T$ gives:

$$Z_T = Z_0 \frac{1 + \rho}{1 - \rho}. \quad (2)$$

The $\epsilon'_r$ is then obtained using (Paulter, 1996):

$$\epsilon_r = \left( \frac{\left[ 120\cosh^{-1}\left( \frac{t_T - t_m}{t_m} \right) - Z_T \right] \pi (t_T - 2t_m)}{Z_T \left[ \pi (t_T - 2t_m) + W\cosh^{-1}\left( \frac{t_T - t_m}{t_m} \right) \right]} \right)^2, \quad (3)$$

where $t_T$ is the total sample thickness and $t_m$ is the metal thickness.

During measurements using a reference short circuit, it was noticed that the short-circuit reflection coefficient, $\rho_{sc}$, was not equal to -1 and that a reflection coefficient offset error, $\rho_{off}$, was present. Accordingly, reflection coefficients obtained were corrected for these two errors (Paulter, 1996):

$$\rho = \frac{\rho_{obs} - \rho_{off}}{\rho_{off} - \rho_{sc}}, \quad (4)$$

where $\rho_{obs}$ is the observed sample reflection coefficient.

The $\epsilon_r$ found with this technique is the average over the frequency range of the measurement. The lower limit of this range is dependent on the duration of the displayed TDR signal. For example, an observation time of 10ns corresponds to a lower limit of 1/10ns or 100MHz. The upper limit is based on the approximation $f = 0.35/t_{fall}$, where $t_{fall}$ is the observed 90 percent to 10 percent transition caused by the impedance discontinuity between the PPTL and the TDR, and f is frequency. So, for a 10ns window and $t_{fall} \approx 35$ ps, the bandwidth is 0.1GHz - 10GHz: this is what is assumed here.

## 3. Results

### 3.a Comparison to frequency domain measurements

Various PPTL samples were prepared and measured using SH1. The results are shown in Table I. The values in curly brackets in the far right column are values obtained from frequency-domain measurement methods performed by either the manufacturer or the National Institute of Standards and Technology's (NIST's) Radio Frequency Technology Division in Boulder, CO. Measurement uncertainties will be discussed later. Samples S8 through S11 show a continuous increase in the extracted $\epsilon'_r$ with increasing number of plies. This increase may be due to an unexpected thickness dependence of the measurement process or to the construction of the PWB itself (Paulter, 1996). Consequently, it may be difficult to ascertain if the apparent ply-dependent $\epsilon'_r$ for S8 to S11 in Table I are real, or a measurement artifact.

### 3.b. Measurement errors and calculated measurement uncertainty

The calculated measurement uncertainties, $u_T$, for the samples of Table I are shown in the far right column of Table II. Note: these uncertainties are the result of an uncertainty analysis (Paulter, 1996), and do not represent measurement repeatability or reproducibility, which will be discussed later. The variables included in the uncertainty analysis were: ρ, $\rho_{sc}$, $\rho_{off}$, $t_T$, $t_m$, W, and $Z_0$. The uncertainty contributions of these variables to $u_T$ are displayed in Table II. The measurement uncertainties presented in Table II represent three standard deviations (3σ). The largest contributors to $u_T$ are uncertainties in $t_m$ and in $\rho_{obs}$. For the data presented in Table II, the values used for $Z_0$, $\rho_{sc}$, and $\rho_{off}$ and their associated 3σ uncertainties were: $Z_0 = 50\ \Omega \pm 0.5\ \Omega$, $\rho_{sc} = -0.994 \pm 3.36 \times 10^{-3}$, and $\rho_{off} = 2.2094 \times 10^{-2} \pm 1.37 \times 10^{-3}$. The 3σ uncertainties for W and $t_T$ were 2.45e-6m (0.0001in) and for $t_m$ was 10 per cent of $t_m$.

The uncertainty in $\rho_{obs}$ includes measurement noise and variations in the physical dimensions of the PPTL, that is, of W(x), $t_T(x)$, and $t_m(x)$, where x is position along the PPTL. Since samples S7 through S17 were prepared using a shear, any imperfections in the shear blade could have significant effects on W(x) and consequently on $\rho_{obs}$. This may explain the larger $u_T$ for S7, which was very narrow (about 800μm wide).

**Table I**
Measured physical parameters, observed reflection coefficient, and extracted $\epsilon_r$ using SH1

| Sample | Reflection coefficient, ρ | Total thickness, $t_T$ (m) | Metal thickness, $t_m$ (m) | Width, W (m) | $\epsilon'_r$ {target} |
|---|---|---|---|---|---|
| S7 (1 ply) | −5.174e−1 ± 1.42e-2 | 1.6586e-4 | 3.43e−5 ± 3.43e-6 | 8.1255e-4 | 5.412 {4.11[c]} |
| S8 (2 ply) | −5.025e−1 ± 8.46e-3 | 2.0371e-4 | 3.43e−5 ± 3.43e-6 | 1.4790e-3 | 3.261 {4.11[c]} |
| S9 (4 ply) | −5.626e−1 ± 5.79e-3 | 3.2182e-4 | 3.43e−5 ± 3.43e-6 | 3.2286e-3 | 3.753 {4.11[c]} |
| S10 (8 ply) | −5.654e−1 ± 9.51e-3 | 5.9055e-4 | 3.43e−5 ± 3.43e-6 | 6.8153e-3 | 3.825 {4.11[c]} |
| S11 (16 ply) | −5.678e−1 ± 1.25e-2 | 1.0950e-3 | 3.43e−5 ± 3.43e-6 | 1.3515e-2 | 3.940 {4.11[c]} |
| S12 | −5.705e−1 ± 9.03e-3 | 1.5305e-3 | 1.72e−5 ± 1.72e-6 | 1.9204e-2 | 4.348 |
| S13 | −5.676e−1 ± 5.01e-3 | 1.4831e-3 | 1.72e−5 ± 1.72e-6 | 1.8964e-2 | 4.111 |
| S14 | −5.907e−1 ± 8.55e-3 | 1.5127e-3 | 6.86e−5 ± 6.86e-6 | 1.8868e-2 | 4.318 {4.384[a]} |
| S15 | −5.833e−1 ± 1.12e-2 | 1.3404e-3 | 3.43e−5 ± 3.43e-6 | 1.0641e-2 | 10.20 {10.2[b]} |
| S16 | −5.595e−1 ± 1.12e-2 | 1.3802e-3 | 3.43e−5 ± 3.43e-6 | 1.3467e-2 | 6.040 {6.15[b]} |
| S17 | −6.049e−1 ± 1.48e-2 | 7.9451e-4 | 3.43e−5 ± 3.43e-6 | 1.4130e-2 | 2.335 {2.2[b]} |

**Notes:**
[a] Measured values obtained by NIST, Boulder, CO; measured at 16GHz;
[b] Manufacturer specification, measured at 10GHz;
[c] Manufacturer specification, measured at 1MHz

**Table II**
Measurement uncertainties using SH1. All uncertainties represent three standard deviations

| Sample | From $\rho_{obs}$ | From $\rho_{sc}$ | From $\rho_{off}$ | From $t_T$ | From $t_m$ | From W | From$Z_0$ | $u_T$ |
|---|---|---|---|---|---|---|---|---|
| **S7 (1 ply)** | 4.50e-1 | 5.65e-2 | 2.04e-2 | 1.40e-1 | 1.38 | 2.75e-2 | 1.16e-1 | 1.47 |
| **S8 (2 ply)** | 1.57e-1 | 3.22e-2 | 1.23e-2 | 9.60e-3 | 6.64e-1 | 7.83e-2 | 6.93e-2 | 6.90e-1 |
| **S9 (4 ply)** | 1.23e-1 | 4.44e-2 | 1.34e-2 | 5.33e-2 | 4.96e-1 | 5.23e-3 | 7.82e-2 | 5.24e-1 |
| **S10 (8 ply)** | 2.23e-1 | 4.54e-2 | 1.35e-2 | 3.38e-2 | 3.31e-1 | 2.57e-3 | 7.90e-2 | 4.10e-1 |
| **S11 (16 ply)** | 3.01e-1 | 4.68e-2 | 1.38e-2 | 2.23e-2 | 2.47e-1 | 1.39e-3 | 8.10e-2 | 4.01e-1 |
| **S12** | 2.39e-1 | 5.19e-2 | 1.51e-2 | 2.44e-2 | 1.87e-1 | 1.06e-3 | 8.88e-2 | 3.22e-1 |
| **S13** | 1.25e-1 | 4.86e-2 | 1.43e-2 | 2.36e-2 | 1.78e-1 | 1.01e-3 | 8.40e-2 | 2.40e-1 |
| **S14** | 2.25e-1 | 5.33e-2 | 1.43e-2 | 1.52e-2 | 3.08e-1 | 1.01e-3 | 8.51e-2 | 3.93e-1 |
| **S15** | 7.14e-1 | 1.28e-1 | 3.53e-2 | 4.92e-2 | 5.79e-1 | 4.32e-3 | 2.09e-1 | 9.53e-1 |
| **S16** | 4.07e-1 | 6.98e-2 | 2.13e-2 | 2.89e-2 | 3.41e-1 | 2.05e-3 | 1.24e-1 | 5.51e-1 |
| **S17** | 2.26e-1 | 3.16e-2 | 7.80e-3 | 1.68e-2 | 1.71e-1 | 7.77e-4 | 4.79e-2 | 2.90e-1 |
| **Average** | 2.91e-1 | 5.53e-2 | 1.65e-2 | 3.79e-2 | 4.44e-1 | 1.14e-2 | 9.66e-2 | 5.68e-1 |

Errors in the measurement of $\rho_{obs}$ may be also caused by:

1. lack of repeatability of sample insertion; and
2. the position of the sample holder center pin with respect to sample center (Paulter, 1996).

The repeatability issue was examined by taking ten consecutive data sets, where a set consisted of a reference (short circuit) and a sample measurement, and comparing the reference and sample data. The mean and 3σ standard deviation of $\rho_{obs}$ for the reference and sample sets were $-9.8987 \times 10^{-1} \pm 3.273 \times 10^{-3}$ and $-5.87579 \times 10^{-1} \pm 2.30 \times 10^{-3}$, which shows that sample insertion contributes negligibly to measurement error. The effect of the position of the center pin on the measurement was also examined. This was done by performing five measurements on a 19mm wide sample where the center pin was placed at different positions relative to the center of the sample for each measurement. Table III shows the measurement results: $\rho_{obs}$ is relatively insensitive to center pin location.

The uncertainty in $t_m$ was based on the Institute for Interconnecting and Packaging Electronic Circuits' (IPC)

**Table III**
Mean and 3σ standard deviation for $\rho_{obs}$

| Center pin position relative to sample center | Reflection coefficient |
|---|---|
| **5mm to the left** | −6.0111e-1 ± 6.15e-3 |
| **2.5mm to the left** | −6.0100e-1 ± 4.20e-3 |
| **Centered** | −6.0074e-1 ± 3.83e-3 |
| **2.5mm to the right** | −6.0077e-1 ± 4.37e-3 |
| **5mm to the right** | −6.0136e-1 ± 6.15e-3 |

**Figure 4**
Dielectric constant measurement results. The upper panel shows the temperature variations during the course of the study and the bottom panel shows the measured dielectric constant for the four different samples as a function of elapsed time, in days

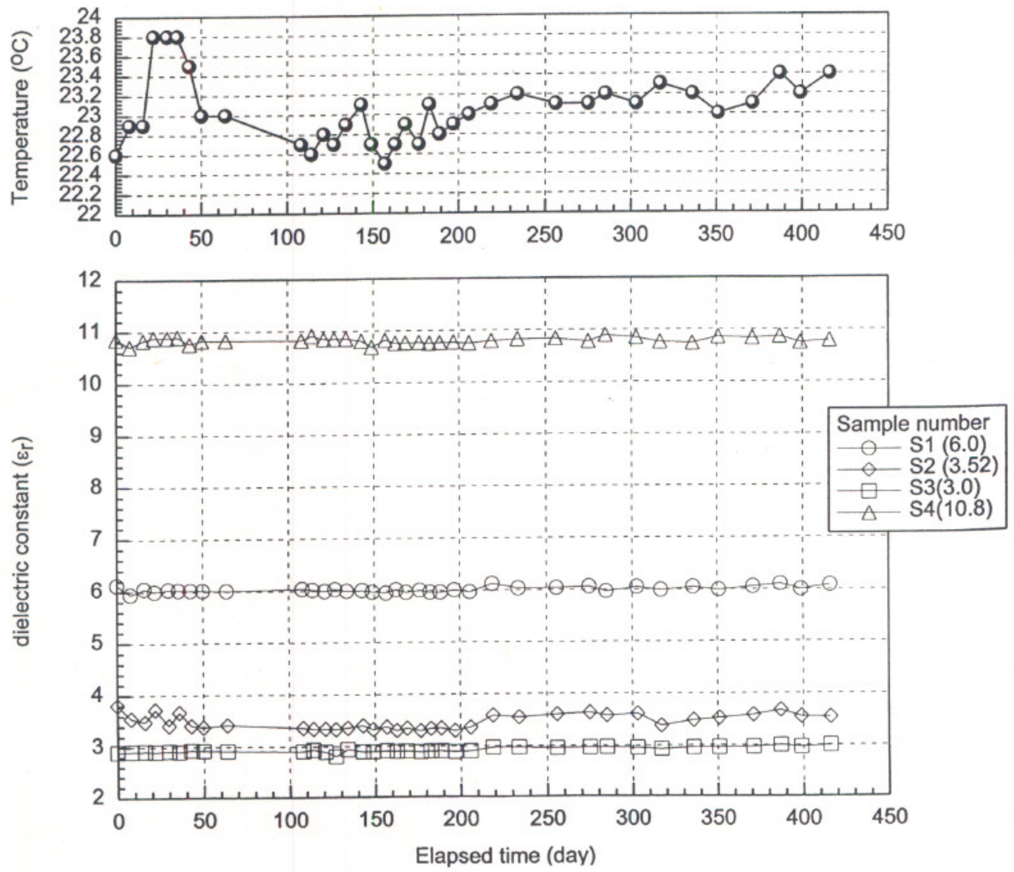

**Table IV**
Dielectric constant measurement results, $\epsilon'_{r,S,n}$ and $\sigma_{S,n}$ for four samples during approximately a 400-day period. The values in the rows with "Day" column entries labeled A through F were taken using the new sample holder. The values in curly brackets in the first row are the $\epsilon'_r$ obtained from frequency domain measurements

| Day | S1 {6.0} | S2 {3.52} | S3 {3.0} | S4 {10.8} | Temperature (°C) |
|---|---|---|---|---|---|
| 0 | 6.123 ± 0.084 | 3.807 ± 0.023 | 2.900 ± 0.014 | 10.860 ± 0.036 | 22.6 |
| 8 | 5.942 ± 0.104 | 3.552 ± 0.050 | 2.908 ± 0.028 | 10.710 ± 0.085 | 22.9 |
| 16 | 6.055 ± 0.118 | 3.485 ± 0.100 | 2.918 ± 0.015 | 10.832 ± 0.053 | 22.9 |
| 22 | 6.002 ± 0.023 | 3.722 ± 0.058 | 2.906 ± 0.028 | 10.884 ± 0.094 | 23.8 |
| 36 | 6.043 ± 0.037 | 3.414 ± 0.025 | 2.920 ± 0.017 | 10.886 ± 0.185 | 23.8 |
| 42 | 6.031 ± 0.092 | 3.667 ± 0.031 | 2.904 ± 0.008 | 10.901 ± 0.141 | 23.8 |
| 49 | 6.026 ± 0.018 | 3.411 ± 0.026 | 2.934 ± 0.022 | 10.764 ± 0.023 | 23.5 |
| 56 | 6.023 ± 0.019 | 3.380 ± 0.024 | 2.925 ± 0.020 | 10.830 ± 0.024 | 23.0 |
| 70 | 6.015 ± 0.018 | 3.420 ± 0.025 | 2.914 ± 0.007 | 10.829 ± 0.029 | 23.0 |
| 128 | 6.042 ± 0.018 | 3.363 ± 0.031 | 2.909 ± 0.004 | 10.822 ± 0.029 | 22.7 |
| 134 | 6.024 ± 0.015 | 3.342 ± 0.032 | 2.935 ± 0.031 | 10.910 ± 0.034 | 22.6 |
| 141 | 5.998 ± 0.026 | 3.344 ± 0.024 | 2.897 ± 0.007 | 10.844 ± 0.084 | 22.8 |
| 147 | 6.032 ± 0.033 | 3.330 ± 0.024 | 2.809 ± 0.008 | 10.846 ± 0.009 | 22.7 |
| 154 | 6.000 ± 0.027 | 3.356 ± 0.028 | 2.943 ± 0.004 | 10.852 ± 0.020 | 22.9 |
| 163 | 6.010 ± 0.024 | 3.402 ± 0.013 | 2.897 ± 0.019 | 10.807 ± 0.025 | 23.1 |
| 169 | 5.977 ± 0.008 | 3.326 ± 0.005 | 2.895 ± 0.001 | 10.686 ± 0.008 | 22.7 |
| 177 | 5.956 ± 0.023 | 3.373 ± 0.031 | 2.909 ± 0.008 | 10.819 ± 0.012 | 22.5 |
| 183 | 6.018 ± 0.013 | 3.303 ± 0.014 | 2.898 ± 0.005 | 10.760 ± 0.006 | 22.7 |
| 189 | 5.968 ± 0.013 | 3.348 ± 0.022 | 2.904 ± 0.010 | 10.767 ± 0.041 | 22.9 |
| 197 | 6.007 ± 0.021 | 3.300 ± 0.017 | 2.889 ± 0.004 | 10.771 ± 0.010 | 22.7 |
| 206 | 5.969 ± 0.003 | 3.360 ± 0.017 | 2.900 ± 0.011 | 10.755 ± 0.010 | 23.1 |
| 219 | 6.125 ± 0.012 | 3.586 ± 0.034 | 2.969 ± 0.009 | 10.795 ± 0.046 | 22.8 |
| 234 | 6.036 ± 0.008 | 3.549 ± 0.024 | 2.969 ± 0.003 | 10.825 ± 0.009 | 22.9 |
| 256 | 6.039 ± 0.007 | 3.600 ± 0.021 | 2.952 ± 0.003 | 10.833 ± 0.056 | 23.0 |
| 275 | 6.064 ± 0.015 | 3.629 ± 0.057 | 2.959 ± 0.011 | 10.776 ± 0.059 | 23.1 |
| 285 | 5.969 ± 0.018 | 3.573 ± 0.043 | 2.962 ± 0.013 | 10.894 ± 0.009 | 23.2 |
| 303 | 6.051 ± 0.011 | 3.607 ± 0.058 | 2.950 ± 0.003 | 10.847 ± 0.025 | 23.1 |
| 317 | 5.993 ± 0.025 | 3.377 ± 0.025 | 2.927 ± 0.010 | 10.759 ± 0.113 | 23.3 |
| 336 | 6.052 ± 0.018 | 3.482 ± 0.085 | 2.955 ± 0.018 | 10.736 ± 0.078 | 23.2 |
| 351 | 5.995 ± 0.031 | 3.524 ± 0.007 | 2.960 ± 0.009 | 10.854 ±0.059 | 23.0 |
| 371 | 6.054 ± 0.021 | 3.580 ± 0.033 | 2.968 ± 0.003 | 10.835 ± 0.021 | 23.1 |
| 387 | 6.104 ± 0.022 | 3.671 ± 0.071 | 3.002 ± 0.007 | 10.865 ± 0.017 | 23.4 |
| 399 | 5.999 ± 0.017 | 3.551 ± 0.031 | 2.969 ± 0.004 | 10.749 ± 0.018 | 23.2 |
| 416 | 6.082 ± 0.029 | 3.541 ± 0.018 | 3.001 ± 0.010 | 10.786 ± 0.125 | 23.4 |
| A | | 3.485 ± 0.017 | | 10.814 ± 0.026 | 22.6 |
| B | | 3.489 ± 0.024 | | 10.800 ± 0.020 | 22.7 |
| C | | 3.508 ± 0.025 | | 10.807 ± 0.020 | 22.8 |
| D | | 3.466 ± 0.030 | | 10.733 ± 0.010 | 22.8 |
| E | | 3.502 ± 0.021 | | 10.794 ± 0.024 | 22.7 |
| F | | 3.505 ± 0.023 | | 10.787 ± 0.024 | 22.8 |

**Table V**
Statistics of the $\epsilon'_{r,S,n}$ and $\sigma_{S,n}$. The two far right columns indicated by S2* and S4* are the results of six (N = 6) measurement sets taken with the new sample holder. The other columns correspond to data from 34 (N 34) measurement sets that were taken with the old sample holder. The values shown in this Table include the coverage factor k [2]: k ≈ 1.01 for N = 34 and k= 1.09 for N = 6

| | S1 | S2 | S3 | S4 | S2* | S4* |
|---|---|---|---|---|---|---|
| $\epsilon'_{r,S} = \frac{1}{N}\sum_{n=1}^{N}\epsilon'_{r,S,n}$ | 6.024 | 3.482 | 2.928 | 10.81 | 3.491 | 10.79 |
| $\sigma_S = \sqrt{\frac{1}{N}}\sqrt{\frac{1}{N}\sum_{n=1}^{N}(\epsilon'_{r,S,n}-\epsilon'_{r,S})^2}$ | 0.006 | 0.023 | 0.006 | 0.009 | 0.007 | 0.012 |
| $\mu_{\sigma,S} = \frac{1}{N}\sum_{n=1}^{N}\sigma_{S,n}$ | 0.029 | 0.033 | 0.011 | 0.047 | 0.027 | 0.023 |
| $\sigma_{\sigma,S} = \sqrt{\frac{1}{N}\sum_{n=1}^{N}(\sigma_{S,n}-\mu_{\sigma,S})^2}$ | 0.027 | 0.021 | 0.008 | 0.043 | 0.007 | 0.005 |

specification ANSI/IPC-MF-150F: the variation in conductor thickness is less than ±5 percent for wrought copper foils and less than ±10 percent for electrodeposited copper foils, and the density of copper is 8.93 gr/cm$^3$ ±1 percent. Using the ANSI/IPC specification gives smaller uncertainties in $t_m$ than that obtainable from simple thickness measurements. However, the effect of copper roughness must still be considered (Paulter, 1996).

The $u_T$ are much greater than the variations in the extracted $\epsilon_r$. To verify this, six additional samples were sheared from the same sheet from which S11 was obtained and then the average extracted $\epsilon'_r$ from these six samples calculated. The average extracted $\epsilon'_r$ was 3.953 and had a 3σ variation of 0.093. This 3σ variation is about four times less than the $u_T$ (0.401) for S11.

### 3.c. Measurement repeatability and reproducibility

The long-term (over a period of one year) reproducibility and short-term (within one hour) repeatability of measurements performed on four different samples, S1 through S4, using sampler holder SH2 are presented. (Definitions of and conditions for repeatability and reproducibility of measurements can be found in Taylor and Kuyatt (1994) or references therein.) Each of the four samples has a different dielectric and physical dimensions and was prepared with a routing tool. Measurements using SH2 resulted in reduced measurement variation compared to measurements using SH1. The samples were placed in an airtight container with a desiccant after day 70.

Measurement sets for S1 through S4 were taken over a period exceeding 400 days. A measurement set for this work consisted of five pairs of acquired waveforms where each pair included a reference waveform and a sample waveform. For each waveform pair for a given sample, a relative dielectric constant value, $\epsilon'_{r,S,n,p}$ (where S refers to the sample number; n to the measurement day, $1 \le n \le N$; and p to the waveform pair, $1 \le p \le 5$) was obtained. Average values and standard deviations of the $\epsilon'_{r,S,n,p}$ ($\epsilon'_{r,S,n}$ and

$\sigma_{S,n}$) were then calculated for each of the N measurement days for each sample to determine short-term measurement repeatability.

Then results of these measurements, the $\in'_{r,S,n}$ and $\sigma_{S,n}$ values, are shown in Figure 4 and Table IV. (The "Day" column labeled "A" through "F" in Table IV represents the measurement days when SH3 was used: the data for days "A" through "F" were taken within 60 days of day 416.) Table V shows the mean values, $\in'_{rS}$, and standard deviations, $\sigma_S$, of the $\in'_{rS,n}$ values; and the mean values, $\mu_{\sigma,S}$, and standard deviations, $\sigma_{\sigma,S}$, of the $\sigma_{S,n}$ values. The values shown in the two rightmost columns in Table V were obtained using SH3; this will be discussed later. The short-term measurement repeatability (1 $\sigma$) varies from about 0.3 percent to about 2.5 percent (see Table IV). The larger deviations are usually caused by one spurious waveform, spurious meaning that the waveform values deviate a few percent relative to the average. Although spurious data may be recognized easily and rejected by an experienced user, this may not be true for a factory floor operator. Consequently, the spurious waveforms were used in computing the average values, $\in'_{rS,n}$, and uncertainties, $\sigma_{S,n}$, that are shown in Table V. The spurious waveforms are probably caused by sample insertion repeatability (Paulter, 1998).

From Table IV and Figure 4 we can also see that measurement variation over the test period is low, especially for sample S3. Sample S2 may have exhibited the largest $\sigma_S$ because it was thin and would sway after being placed in the sample holder, which would affect the electrical location of the sample within the sample holder (Paulter, 1998).

The $\mu_{\sigma,S}$ and $\sigma_{\sigma,S}$ are used as indicators of measurement repeatability: $\mu_{\sigma,S}$ indicates the average variability in measurement values and $\sigma_{\sigma,S}$ indicates the scatter or variation in measurement repeatability. For example, if $\sigma_{\sigma,S} >> \mu_{\sigma,S}$ (the scatter in measurement repeatability is greater than the average repeatability), then spurious waveforms probably existed and were used in the calculation of $\in'_r$. Consequently, it may be possible to improve the measurement process by removing the cause of the spurious waveform. On the other hand, if $\sigma_{\sigma,S} << \mu_{\sigma,S}$, then measurement repeatability improvement is unlikely. However, for S1 through S4, $\sigma_{\sigma,S} \approx \mu_{\sigma,S}$, which implies measurement improvement is possible (to be discussed shortly). The long-term reproducibility can be obtained from $\sigma_S$ in Table V: 0.1 per cent for S1, 0.7 percent for S2, 0.2 percent for S3, and 0.1 percent for S4. The large $\sigma_s$ for S2 was probably caused by poor sample holder design, as will be discussed later. The $\sigma_s$ also provides an indication of drift in the measurement process, and the $\sigma_s$ values presented here indicate very low drift.

To reduce the scatter in the measurement repeatability, the sample holder SH3 was designed. The knife edge contacts of SH3 were expected to reduce possible contact repeatability problems at the base plate and sample. The rows labeled A through F in Table IV and the two rightmost columns of Table V show the results of the six measurement sets taken with SH3 for S2 and S4. We can see from Table V that SH3 reduced the scatter in measurement repeatability significantly for S2 and S4 and reduced $\sigma_S$ of S2 to values similar to those for the other samples. However, the average variation in the measurement, indicated by $\mu_{\sigma,S}$, did not change when using SH3. Additional measurements indicated that $\mu_{\sigma,S}$ is limited by oscilloscope repeatability (Paulter, 1998).

## Conclusions

A TDR based measurement method has been described for determining the real part of the permittivity of the dielectrics of printed wiring board materials. The measurement system is inexpensive and easy to use. Sample preparation is easy and measurements are insensitive to the position of the sample within the sample holder. The long-term reproducibility and short-term repeatability of the measurement system are better than 0.5 percent. The measurement results are within 2 percent of those reported by frequency-domain methods using the poorest performing sample holder (SH1) and within 1 percent for the best performing sample holder (SH3).

## References

Baker-Jarvis, J., Janezic, M.D., Grosvenor, J.H. and Geyer, R.G. (1993), *Transmission/Reflection and Short-Circuit Line Methods for Measuring Permittivity and Permeability, National Institute of Standards and Technology Technical Note 1355-R*, US Government Printing Office, Washington, DC.

Boned, C. and Peyrelasse, J. (1982), "Automatic measurement of complex permittivity (from 2MHz to 8GHz) using time domain spectroscopy", *J. Phys. E: Sci. Instrum.*, Vol. 15, p. 534.

Cole, R.H. (1975), "Evaluation of dielectric behavior by time domain spectroscopy. 1. Dielectric response by real time analysis", *J. Phys. Chem.*, Vol. 79, p. 1459.

Fellner-Feldegg, H. (1969), "The measurement of dielectrics in the time domain", *Journal of Phys. Chem.*, Vol. 73, March, p. 616.

Kent, G. (1991), "A dielectrometer for the measurement of substrate permittivity", *Microwave Journal*, December, p. 72.

Lightart, L.P. (1983), "A fast computational technique for accurate permittivity determination using transmission line methods", *IEEE Trans. Microwave Theory Tech.*, Vol. MTT-31, March, p. 249.

Nicolson, A.M. and Ross, G.F. (1970), "Measurement of the intrinsic properties of materials by time-domain techniques", *IEEE Trans. Instrum. Meas.*, Vol. IM-19, November, p. 377.

Paulter, N.G. (1996), "A fast and accurate method for measuring the dielectric constant of printed wiring board materials", *IEEE Trans. CHMT-C*, Vol. 19, July, p. 214.

Paulter, N.G. (1998), "Long-term repeatability of a TDR-based printed wiring board dielectric constant measurement system", *IEEE Trans. Instrum. Meas.*, December.

Stuchly, S.S., Sibbald, C.L. and Anderson, J.M. (1994), "A new aperture admittance model for open-ended waveguides", *IEEE Trans. Microwave Theory Tech.*, Vol. 42, February, p. 192.

Taylor, B.N. and Kuyatt, C.E. (1994), "Guidelines for evaluating and expressing the uncertainty of NIST measurement results", *NIST Technical Note 1297*, 1994 edition, US Government Printing Office, Washington, DC.